Molecular & Cellular Toxicology (2020) 16:1–11
https://doi.org/10.1007/s13273-019-00052-x

ORIGINAL ARTICLE

Apoptosis and necroptosis-inducing effects of arctigenin on nasal septum carcinoma RPMI-2650 cells in 2D and 3D culture

Yoon-Jin Lee[1] · Kwan-Sik Park[1] · Byoung Joon Baek[2] · Kyong-Ae Lee[3] · Sang-Han Lee[1]

Accepted: 7 November 2019 / Published online: 3 December 2019

Abstract

Backgrounds Arctigenin derived from the seeds of *Arctium lappa* Linnaeus is known as an anticancer drug candidate by targeting various pathways involved in anticancer therapy.

Methods Using 2D monolayer and 3D spheroid culture systems in nasal septum carcinoma RPMI-2650 cells, the effects of arctigenin and dexamethasone on cell viability, ROS levels, ATP level, mitochondrial function, apoptosis and necroptosis were examined.

Results The combination treatment of both compounds induced strong cytotoxicity, accompanied by increases of sub-G_0/G_1 peak, annexin V-PE-positive cells, and ROS levels, loss of mitochondrial membrane potential, and decrease of cellular ATP content. These changes were observed as simultaneous induction of DNA damage, apoptosis, and necroptosis. A series of changes by arctigenin and dexamethasone were efficiently restored by decreasing ROS levels or supplementing ATP. Treatment of 3D spheroids with arctigenin and dexamethasone decreased cell viability in the spheroids, but it was slightly resistant than cells under 2D conditions. In addition, this phenomenon was accompanied by an increase in mediators for both apoptosis and necroptosis.

Conclusion Results of this study suggest that the apoptosis and necroptosis-inducing effects of arctigenin are associated with ATP depletion due to oxidative mitochondrial dysfunction.

Keywords Arctigenin · Dexamethasone · Necroptosis · Apoptosis · DNA damage · Oxidative stress · ATP

Introduction

Cancers of the nasal cavity are extremely uncommon neoplasms, comprising < 1% of all head and neck cancers (Allen et al. 2008). Among these, malignancies of the nasal septum are rare, accounting for about 9% of all cancers in the nasal cavity (Fradis et al. 1993). These tumors are considered fatal if they are not diagnosed or treated early (McGuirt and Thompson 1984). The standard treatment for these carcinomas often involves surgical resection followed by postoperative radiotherapy with or without chemotherapy. Cyclophosphamide, vincristine, cisplatin, and doxorubicin are the most used drugs in the treatment of cancers of the nasal cavity. Many researchers have attempted to discover new therapies for controlling nasal septum carcinoma.

The use of dietary phytochemicals as adjuvants has been shown to play a role in improving the efficacy of chemotherapeutic drugs due to their multitargeted properties and low toxicity to normal tissues (Davatgaran-Taghipour et al. 2017). Among these, arctigenin (ATG), a dibenzylbutyrolactone lignin extracted from the seeds of *Arctium lappa*, has shown anticancer activity against various cancers (Li et al. 2016; Feng et al. 2017; Xu et al. 2017). ATG can induce cell cycle arrest and mitochondrial caspase-independent apoptosis by increasing ROS (Li et al. 2016). It can also inhibit the growth of MDA-MB-231 breast cancer xenograft tumors without causing obvious toxic side effects (Feng et al. 2017). In addition, ATG suppresses migration and invasion of cancer cells by inhibiting TGF-β-induced

✉ Sang-Han Lee
m1037624@sch.ac.kr

[1] Department of Biochemistry, College of Medicine, Soonchunhyang University, Cheonan 31151, Republic of Korea

[2] Department of Otolaryngology–Head and Neck Surgery, Cheonan Hospital, College of Medicine, Soonchunhyang University, Cheonan 31151, Republic of Korea

[3] Department Food Science and Nutrition, Soonchunhyang University, Asan 31538, Republic of Korea

epithelial-mesenchymal transition (Xu et al. 2017). Moreover, ATG can inhibit complex I in the mitochondrial respiration chain, resulting in the induction of preferential necrosis of glucose-starved A549 tumor cells (Gu et al. 2012). Recently, several groups have conducted phase I trials of ATG as an inhibitor of mitochondrial complex I in patients with gemcitabine-refractory pancreatic cancer and shown the possibility of its clinical application due to high bioavailability, good safety profile, and promising chemotherapeutic responses (Fujioka et al. 2018; Ikeda et al. 2016). Although ATG might have potential benefits in the treatment of a variety of cancers, the anticancer activity of ATG on nasal septum carcinoma cells has not been established yet.

Glucocorticoids can regulate biological processes such as cell proliferation, differentiation, development and inflammation (Dorscheid et al. 2001). They are known to be able to decrease symptoms associated with cancer treatment such as edema, inflammation, pain, lack of appetite, and electrolyte imbalance in many clinical situations (Ioannidis et al. 2000). Dexamethasone (DMS), a synthetic glucocorticoid, can prevent growth of many types of tumor cells, including hepatoma (Li et al. 2010), osteosarcoma (Yamamoto et al. 2002), lung cancer (Greenberg et al. 2002), and breast cancer cells (Wang et al. 2007). Dorscheid et al. have reported that DMS can induce apoptosis of airway epithelium in experiments using primary and immortalized cell lines (Dorscheid et al. 2001). Although apoptosis has been shown to be an important mechanism involved in the effect of glucocorticoid treatment, cellular responses and molecular events induced by this drug remain unclear.

Necroptosis is a type of programmed necrosis caused by the sequential activation of a series of signals. It is initiated by the formation of the necrosome through the interaction of receptor-interacting protein (RIP) 1 and RIP3. RIP3, activated by RIP1 in the necrosome, then phosphorylates and activates the mixed lineage kinase domain-like (MLKL) protein responsible for necroptosis (Qin et al. 2019). Although the complete mechanism underlying necroptosis is not completely understood yet, mitochondrial dysfunction is known to play a role in inducing necroptosis (Zhu et al. 2018). In this process, high level of reactive oxygen species (ROS) has been implicated in the execution of necroptosis. Necroptosis contributes to cancer cell death induced by chemotherapeutic agents in apoptosis-resistant tumors. Therapeutic strategies to induce necroptosis in cancer cells have shown great potential in chemotherapy.

The objective of this study was to investigate cytotoxic effects of ATG and DMS, either alone or in combination, on nasal septum carcinoma cells and examine expression levels of biochemical marker proteins related to apoptosis, necroptosis, and DNA damage. Our results provide evidence that combination treatment with both ATG and DMS (ATG/DMS) simultaneously can induce apoptosis and necroptosis by ATP depletion due to oxidative mitochondrial dysfunction.

Materials and methods

Cell culture

The human nasal septum carcinoma cell line RPMI-2650 was purchased from the American Type Culture Collection (ATCC, Manassas, USA). The cells were grown to 70% confluence in EMEM (ATCC) supplemented with 10% fetal bovine serum, 1 mM glutamine, 100 units of penicillin/mL and 100 µg of streptomycin/mL before treatment.

MTT assay

For cell viability analysis, approximately 5×10^3 cells per well were seeded in 96-well culture plates and maintained in EMEM (Welgene, Korea) containing vehicle (0.1% dimethylsulfoxide), ATG and/or DMS for the indicated time, and then exposed to 3-(4,5-dimethylthiazol-2-yl)-2,5-diphenyltetrazolium bromide (Sigma-Aldrich, Germany) for 4 h at 37 °C. Absorbance values were measured at 540 nm using a GloMax-Multi Microplate Multimode Reader (Promega Corporation, USA). Percentage of viable cells was determined by comparison with the results of vehicle-treated control cells (100%) for each treatment and time point.

Spheroid culture and viability assay

The cells were seeded in Ultra-Low attachment 96-well plate at a density of 10^4 cells per well, after which the plates were centrifuged at 1000 rpm for 10 min to facilitate clustering of the cells into the wells, as described by Chambers et al. (Chambers et al. 2014), and maintained in the complete EMEM. Spheroids were treated with ATG for 48 h. Phase contrast images were taken using a Leica inverted microscope. Spheroid viability was determined using the Enhanced cell viability assay kit (CellVia, Seoul, Korea), according to the manufacturer's instructions. After treatment, 10 uL of Cellvia solution was added per well, incubated at 37 °C for 1 h, and mixed by shaking for 1 min. Formazan formed in living cells was measured with a spectrophotometer at 450 nm in a GloMax-Multi Microplate Multimode Reader (Promega Corporation).

Spheroid staining

Cells were incubated with fluorescein diacetate (FDA, 5 µg/mL) and propidum iodide (PI, 10 µg/mL) for 5 min in the dark to stain live and dead cells, respectively. In vitality staining of spheroids, FDA is converted to the green

fluorescent metabolite in live cells, whereas PI binds to DNA by passing through disordered areas of dead-cell membranes. Spheroids were imaged using a Leica EL6000 fluorescence microscope and LAS version 4.3 software (Leica Microsystems Inc., IL, USA).

Cell cycle analysis

Percentages of cells in each phase in the cell cycle were determined by quantification of DNA content in cells stained with PI. Trypsinized cells (10^6 cells/mL) were then pelleted using centrifugation at 500×*g* for 7 min at 4 °C, fixed overnight in 70% ice-cold ethanol at − 20 °C, and incubated with the Muse™ cell cycle reagent (Merck Millipore, USA). Data for 10^4 single-cell events were analyzed using MACSQuant Analyzer and MACSQuantify™ version 2.5 software (MiltenyiBiotec GmbH, Germany).

Annexin V-PE binding assay

The distribution of apoptotic-cells was determined using the Muse™Annexin V & Dead cell assay kit (MCH100105; Merck KGaA). The kit contains phycoerythrin (PE), a fluorescent-dye that is conjugated to the annexin V to detect phosphatidylserine on the outer layer of apoptotic cell membrane, and 7-amino-actinomycin D (7-AAD), a dead-cell marker. Briefly, 10^5 cells per well were seeded in 6-well culture plates and treated with ATG alone or in combination with DMS for the indicated time at 37 °C in EMEM. Cells were then trypsinized, collected on culture media mixed with the Muse™Annexin V & Dead-Cell reagent, and analyzed using the Muse™ Cell Analyzer (Merck KgaA).

Western blot analysis

Total cell lysates were extracted with a 1 × RIPA buffer. Cell lysates containing 40 µg of protein were separated on a 4–12% NuPAGE gel (Thermo Fisher Scientific, Inc., USA) and transferred to a polyvinylidene fluoride membrane (GE Healthcare Life science, Germany). The blots were probed with primary and secondary antibodies coupled to horseradish-peroxidase (HRP) for protein detection. The antigen–antibody complex was visualized using the enhanced chemiluminescence (ECL, Cyanagen Srl, Italy) detection kit and X-ray film. The membrane was stripped using stripping buffer [100 mM β-mercaptoethanol, 2% sodium dodecyl sulfate, and 62.5 mM Tris–HCl at pH of 6.7] and reprobed with anti-β-actin antibody (Sigma-Aldrich) that served as the loading control. Primary Antibodies (MLKL, p-MLKL, RIP3, p-RIP3, p-ATM^{Ser1981}, p-ATR^{Ser428}, p-CHK1^{Ser345}, p-CHK2^{Thr68}, p-histone H2A.X, BAX, Bcl-2, caspase-3, and cleaved caspase-3) for Western blot analysis were purchased from Cell Signaling Technology, Inc. (Danvers, USA).

Measurement of intracellular ROS

The level of reactive oxygen species (ROS) was determined by measuring the fluorescence intensity of 2′,7′-dichlorodihydrofluorescein diacetate (DCF-DA, Sigma-Aldrich). Briefly, 10^5 cells per well were seeded in 6-well culture plate and pretreated with 5 mM *N*-acetylcysteine (NAC) for 2 h at 37 °C prior to treatment with ATG alone or in combination with DMS for an additional 48 h. After cells were trypsinized, they were harvested by centrifugation at 500×*g* for 7 min and resuspended in serum-free EMEM containing 10 µM DCF-DA for 30 min at 37 °C in the dark. Cells were then washed twice with 1 × PBS and immediately analyzed using MACSQuant Analyzer flow cytometer and MACSQuantify™ software version 2.5 (MiltenyiBiotec GmbH). Fluorescence intensities were detected using a 530 nm bandpass filter, and each measurement was based on an average fluorescence intensity of 10,000 cells.

Measurement of mitochondrial membrane potential

Approximately 5×10^4 cells per well were seeded in 6-well culture plates and pretreated with 5 mM NAC for 2 h at 37 °C prior to treatment with ATG alone or in combination with DMS for 48 h. After cells were trypsinized, they were harvested by centrifugation at 500×*g* for 7 min at 4 °C, washed twice with 1 × PBS, and stained with serum-free EMEM containing Rhodamine 123 (final concentration, 30 nM) for 30 min at 37 °C. Following incubation, cells were washed twice with 1 × PBS and resuspended in 1 × PBS. Fluorescence intensities were measured and analyzed using MACSQuant analyzer flow cytometer and MACSQuantify™ software version 2.5 (MiltenyiBiotec GmbH).

Measurement of ATP content

Cellular ATP levels were measured using the CellTiter-Glo-luminiscent cell viability assay kit (Promega Corporation). Briefly, 5×10^3 cells per well were seeded in 96-well culture plates and pretreated with 5 mM NAC for 2 h at 37 °C prior to treatment with ATG/DMS for an additional 48 h. After incubation, the CellTiter-Glo reagent (100 µL/well) was added to the cell culture, placed in a shaker for 2 min, and incubated at room temperature for 10 min to induce complete lysis. Luminescence values were measured using the GloMax-Multi Microplate Multimode Reader (Promega). Data were determined by comparison with the results of vehicle-treated control cells (100%) for each treatment and time point.

Statistical analysis

Statistical comparisons were performed using a one-way analysis of variance, followed by Tukey's post hoc correction for multiple comparisons using the SPSS version 17.0 software package (SPSS, Inc., USA). Data are expressed as mean ± standard deviation (S. D.) for three independent experiments. $*P < 0.05$ was considered statistically significant compared with each control group.

Results

Arctigenin or dexamethasone inhibits the viability of RPMI-2650 cells

Nasal septum carcinoma cells, RPMI-2650, were treated with various concentrations of ATG or DMS for 24, 48, and 72 h to evaluate the effects of these two compounds on cell viability. Decrease in cell viability by treatment with ATG or DMS alone was concentration and time dependent. At the same indicated concentrations, the survival curves of cells treated with ATG showed a steeper trend than those treated with DMS (Fig. 1a). Based on the results of cell viability, concentrations that resulted in cell viability of 75% or more at 48 h treatment (5 μM for ATG and 12.5 μM for DMS) were used in the subsequent experiments. Flow cytometric analysis with PI staining was performed to determine whether ATG or DMS could induce cell death. As shown in Fig. 1b, ATG or DMS alone induced an increase in the sub-G_0/G_1 peak of the cell cycle, indicating cell death. In double staining with annexin V-PE and 7-AAD, ATG or DMS induced a clear reduction in annexin V-PE-negative/7-AAD-negative (viable) cells, but a significant increase in annexin V-PE-positive/7-AAD-negative (apoptosis) cells or annexin V-PE-positive/7-AAD-positive (necrosis) cells (Fig. 1c).

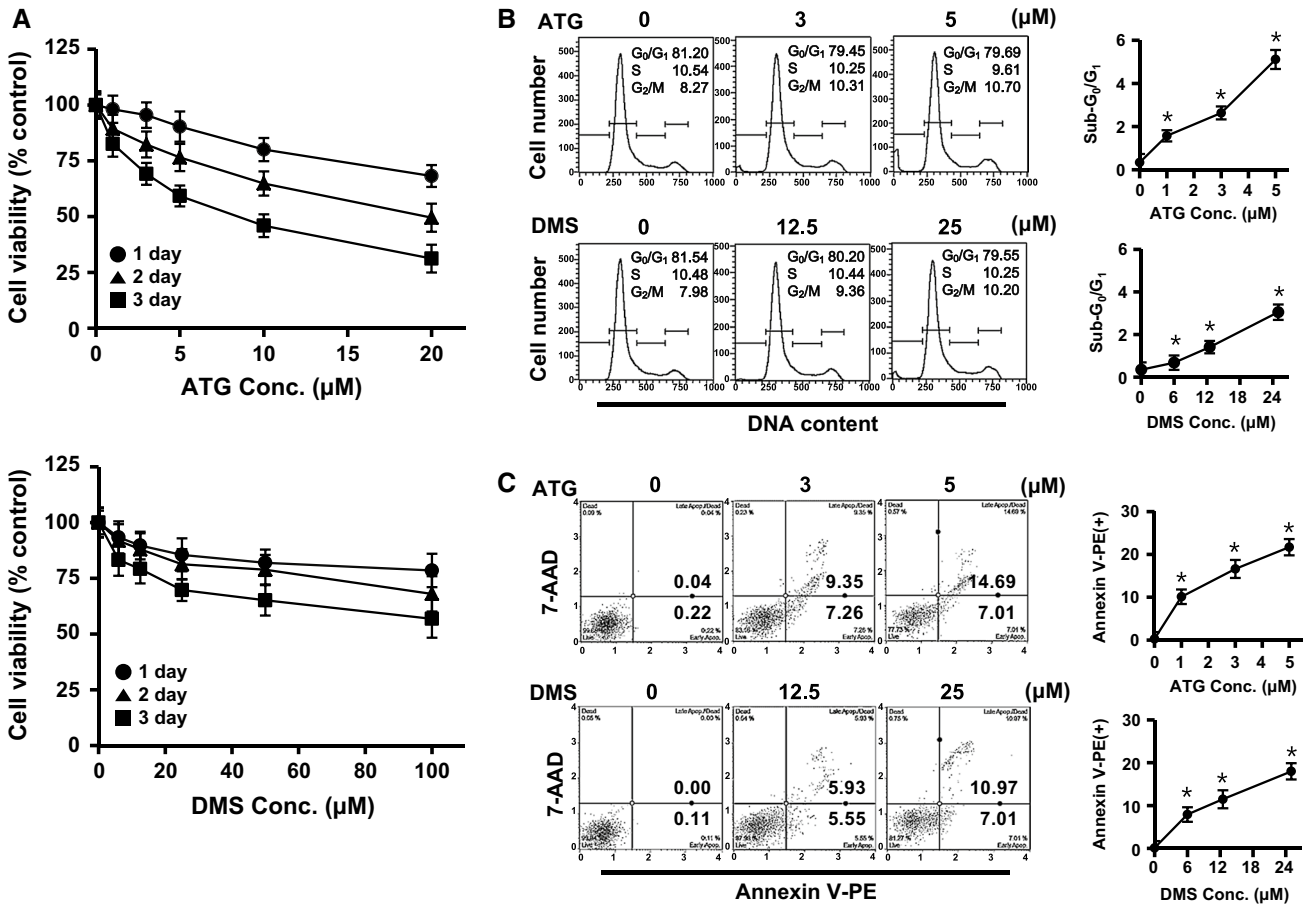

Fig. 1 Effects of arctigenin or dexamethasone on cell growth in RPMI-2650 cells. **a** Cells were treated with increasing concentration of ATG (0, 1.25, 2.5, 5, 10 and 20 μM) or DMS (0, 6.25, 12,5, 25, 50, and 100 μM) for 24 h, 48 h, and 72 h. The percentage of viable cells was measured by MTT assay. (**b** and **c**) Cells were treated with indicated concentrations of ATG or DMS for 48 h. Cell cycle analysis was performed after staining cells with propidium iodide (**b**). Apoptotic cell fraction was analyzed using annexin V-PE binding assay (**c**). Error bars represent the mean ± SD of three independent experiments. *ATG* arctigenin, *DMS* dexamethasone; *7-AAD* 7-amino-actinomycin D. $*P < 0.05$ compared with non-treatment controls

Next, we investigated whether cell death induced by ATG or DMS was accompanied by an increase in cellular ROS levels. Flow cytometry showed a clear increase in intracellular ROS levels after treatment ATG or DMS in a dose-dependent manner (Fig. 2a). ROS is known to be mainly produced in mitochondria. Thus, we analyzed the integrity of mitochondrial function with a flow cytometry using rhodamine-123, a fluorescent dye. Results showed that ATG or DMS induced a concentration-dependent loss of mitochondrial membrane potential (ΔΨm). Treatment with ATG (5 μM) or DMS (12.5 μM) alone resulted in a significant reduction in fluorescence intensity (by approximately 23.15% and 18.16%, respectively) compared to non-treatment control (Fig. 2b). To investigate cytotoxic effects of ATG or DMS on apoptosis and/or necroptosis, expression levels of apoptosis- and necroptosis-related proteins were examined by Western blotting. As shown in Fig. 2c, ATG or DMS alone induced increased levels of proapoptotic proteins such as Bax and cleaved caspase-3, and decreased levels of antiapoptotic protein Bcl-2. In addition, ATG or DMS increased the levels of necroptosis markers p-RIP3 and its downstream target p-MLKL, although their intensities were much stronger in cells treated with ATG than those in DMS-treated cells.

Arctigenin alone or in combination with dexamethasone simultaneously induces apoptosis and necroptosis

The sensitivity of RPMI-2650 cells to ATG/DMS was investigated using MTT assay following treatment with these compounds for 24, 48, and 72 h. Exposure of cells to 5 μM ATG and 12.5 μM DMS in combination for 48 h resulted in a significant decrease in cell viability (58.3%) compared to ATG (76.5%) or DMS (88.2%) alone (Fig. 3a). In addition, ATG/DMS increased the levels of apoptosis- or necroptosis-related proteins more than ATG or DMS alone (Fig. 3b). To further confirm that ATG/DMS could concurrently changes levels of apoptosis- or necroptosis-related proteins, prior to ATG/DMS treatment cells were pretreated with Q-VD-Oph-1 as a pan-caspase inhibitor for apoptosis or necrostatin-1 as a RIP1 inhibitor for necroptosis. Pretreatment with inhibitors for 48 h resulted in decreased levels of cleaved caspase-3, p-RIP3, and p-MLKL (Fig. 3c) with recovery of cell viability (Fig. 3d) compared to combination treatment of the two compounds. Interestingly, addition of ATP effectively reversed the levels of cleaved caspase-3, p-RIP3, and p-MLKL as well as the decrease in cell viability by ATG/DMS. This suggests that ATG/DMS targets mitochondria as

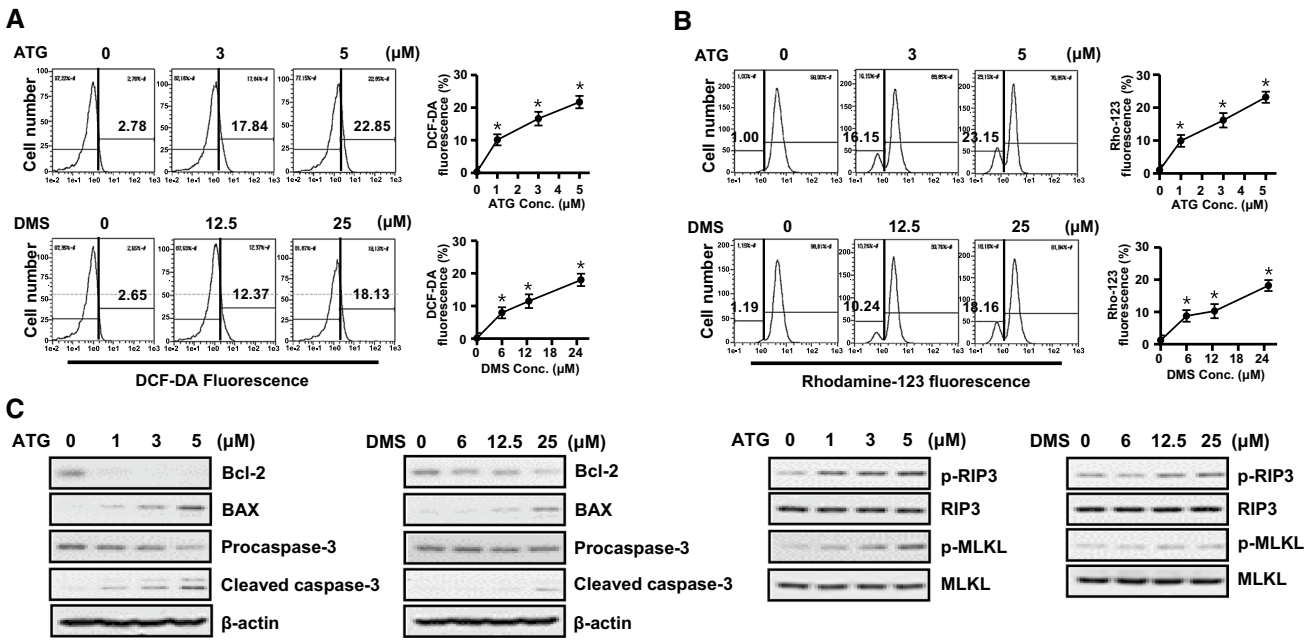

Fig. 2 Effects of arctigenin or dexamethasone on ROS and mitochondrial function in RPMI-2650 cells. Cells were treated with indicated concentration of ATG or DMS for 48 h. **a** Cellular ROS levels were measured after staining cells with DCF-DA (10 μM). **b** ΔΨm was measured after staining cells with 30 nM of Rhodamine123. **c** Levels of apoptosis- and necroptosis-related proteins were measured by Western blotting. Error bars represent the mean ± SD of three independent experiments. *ATG* arctigenin, *DMS* dexamethasone. $^{*}P < 0.05$ compared with non-treatment controls

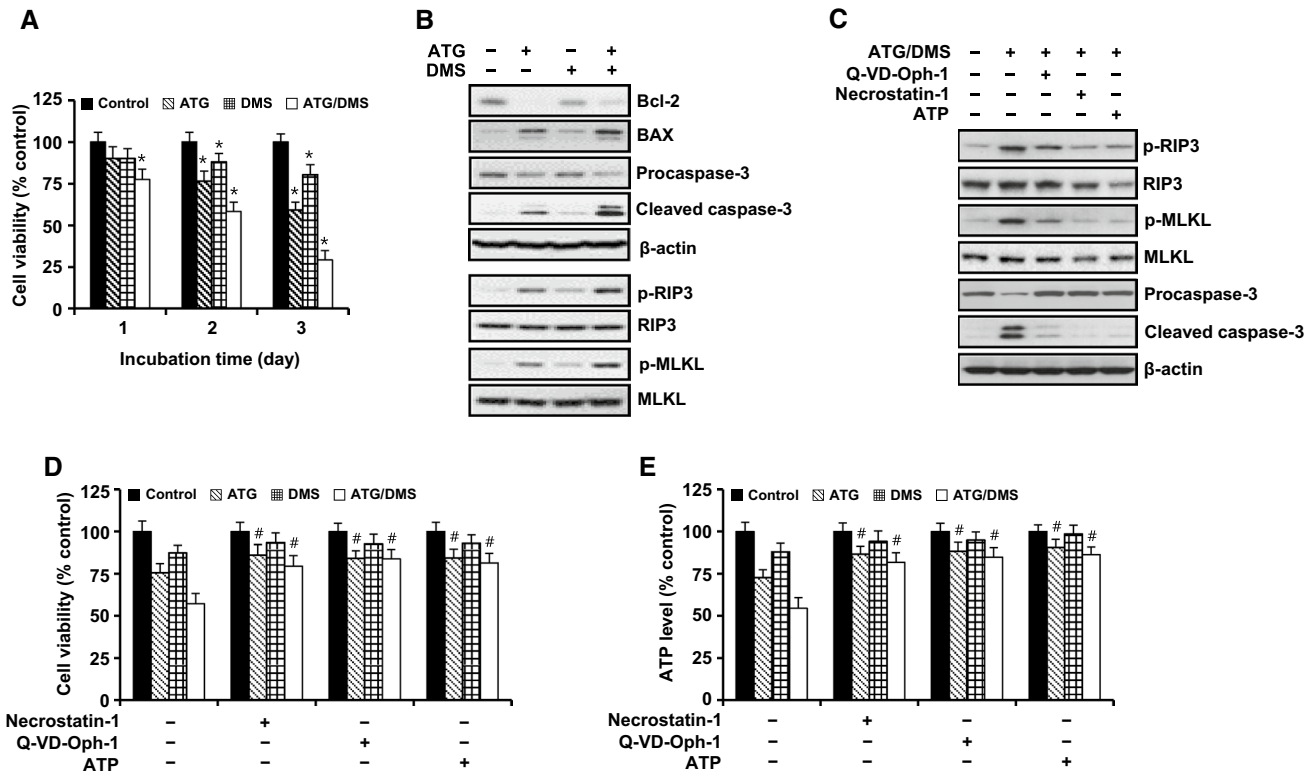

Fig. 3 Effects of the combination treatment of arctigenin and dexamethasone on cell viability and cell death in RPMI-2650 cells. **a** Cells were treated with ATG (5 μM) and DMS (12.5 μM), alone or in combination, for the indicated times. The percentage of viable cells was measured by MTT assay. **b** Cells were treated with ATG (5 μM) and DMS (12.5 μM) alone or in combination for 48 h. Levels of apoptosis- and necroptosis-related proteins were measured by Western blotting. **c**–**e** Cells were pretreated with necrostatin-1 (25 μM), Q-VD-Oph-1 (10 μM), and ATP (1 mM) 2 h prior to combination treatment with ATG (5 μM) and DMS (12.5 μM) for 48 h. Levels of apoptosis- and necroptosis-related proteins were measured by Western blotting (**c**). Percentage of cell viability was measured by MTT assay (**d**). Intracellular ATP levels were measured by CellTiter-Glo luminescent cell viability assay (**e**). Error bars represent the mean ± S.D. of three independent experiments. *ATG* arctigenin, *DMS* dexamethasone. $^{*}P < 0.05$ compared with non-treatment controls. $^{\#}P < 0.05$ compared with respective controls without pretreatment

the cell's supply of ATP. Next, we evaluated if ATP metabolism affected combined effects of ATG/DMS on apoptosis and necroptosis. Notably, we found that the ATP levels were significantly reduced in cells treated with ATG/DMS, but were effectively rescued in cells pretreated with Q-VD-Oph-1 or necrostatin-1 (Fig. 3e).

ROS is required for cell death induced by arctigenin and dexamethasone

To investigate the role of ROS in apoptosis and necroptosis induced by ATG/DMS, a ROS scavenger *N*-acetylcysteine (NAC) was used to reduce intracellular ROS levels. Pretreatment with NAC for 2 h significantly recovered a series of events induced by ATG/DMS, including a decrease in the cell viability (Fig. 4a, b), an increase in annexin V-PE-positive/7-AAD-negative cells or annexin V-PE-positive/7-AAD-positive cells (Fig. 4c), accumulation of cells at sub-G_0/G_1 phase of cell cycle (Fig. 4d), increased levels of Bax, cleaved caspase-3, p-RIP3, and p-MLKL proteins, and a decreased level of Bcl-2 protein (Fig. 4e).

Flow cytometry revealed that pretreatment with NAC reduced increased ROS levels and ΔΨm loss caused by ATX/DMS (Fig. 5a, b). To evaluate the effects of ATG/DMS on DNA damage, phosphorylation levels of DNA damage response markers such as ATM, ATR, CHK1, CHK2, and histone H2A.X were investigated after treatment with ATG/DMS. As shown in Fig. 5c, the levels of p-ATM^{Ser1981} and p-ATR^{Ser428} as well as their downstream effectors, p-CHK-1^{Ser345} and p-CHK2^{Thr68}, increased, which were accompanied by an increase of the p-Histone H2A.X^{Ser139} as a marker for DNA double-strand breaks. However, pretreatment with NAC effectively restored increases of ATG/DMS-induced DNA damage markers.

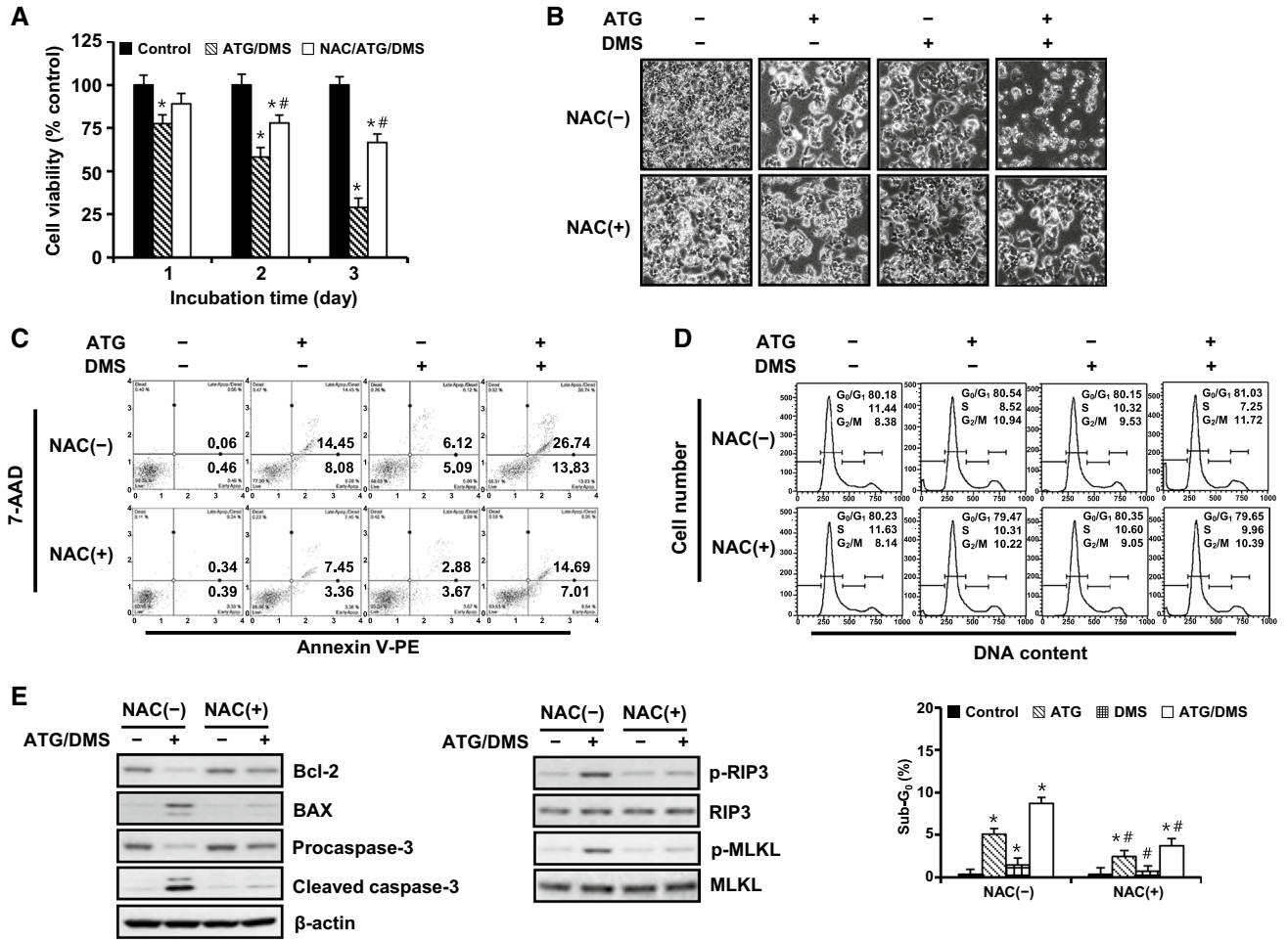

Fig. 4 Effects of pretreatment with *N*-acetylcysteine following combination treatment of arctigenin and dexamethasone on cell growth and cell death in RPMI-2650 cells. **a** Cells were pretreated with *N*-acetylcysteine (5 mM) prior to treatment with ATG (5 μM) and DMS (12.5 μM) alone or in combination for the indicated times. The percentage of viable cells was measured by MTT assay. **b–e** Cells were treated with ATG (5 μM) and DMS (12.5 μM), alone or in combination, for 48 h. Cell morphology was observed under a light microscope (**b**). Apoptotic cell fraction was analyzed using annexin V-PE binding assay (**c**). Cell cycle analysis was measured after staining cells with propidium iodide (**d**). Levels of apoptosis- and necroptosis-related proteins were measured by Western blotting (**e**). *ATG* arctigenin, *DMS* dexamethasone, *ATG/DMS* combination treatment of arctigenin and dexamethasone, *NAC N*-acetylcysteine. $^{*}P<0.05$ compared with non-treatment controls. $^{\#}P<0.05$ compared with respective controls without NAC pretreatment

To confirm whether the results of the 2D monolayer culture are consistent in 3D culture, the RPMI-2650 cells-derived spheroids were treated with ATG/DMS for 48 h, after which spheroids were incubated with FDA and PI to stain live and dead cells, respectively. As shown in Fig. 6a, b, ATG/DMS increased PI(+) area showing necrotic cell death with decreased cell viability in spheroids, but it was slightly resistant than cells under 2D conditions. To characterize the nature of cell death, we analyzed the effects of ATG/DMS on apoptotic and necroptotic mediators. As shown in Fig. 6c, ATG/DMS showed the increased levels of cleaved caspase-3, BAX, p-RIP3 and p-MLKL proteins, and the decreased level of Bcl-2. These findings were restored by pretreatment with NAC.

Discussion

In this study, we evaluated anticancer effects of ATG and DMS alone or in combination on cell growth, cell death, ROS, mitochondrial function, and DNA damage in nasal septum carcinoma RPMI-2650 cells. Our data provided a mechanistic explanation that ATG/DMS-induced cytotoxicity was associated with oxidative mitochondrial damage and subsequent ATP depletion that led to simultaneous induction of apoptosis and necroptosis, ultimately resulting in significant death of RPMI-2650 cells. This study demonstrates for the first time that ATG/DMS kills RPMI-2650 cells through necroptosis as well as apoptosis in both 2D and 3D cultures. ATG/DMS-induced cytotoxicity was demonstrated

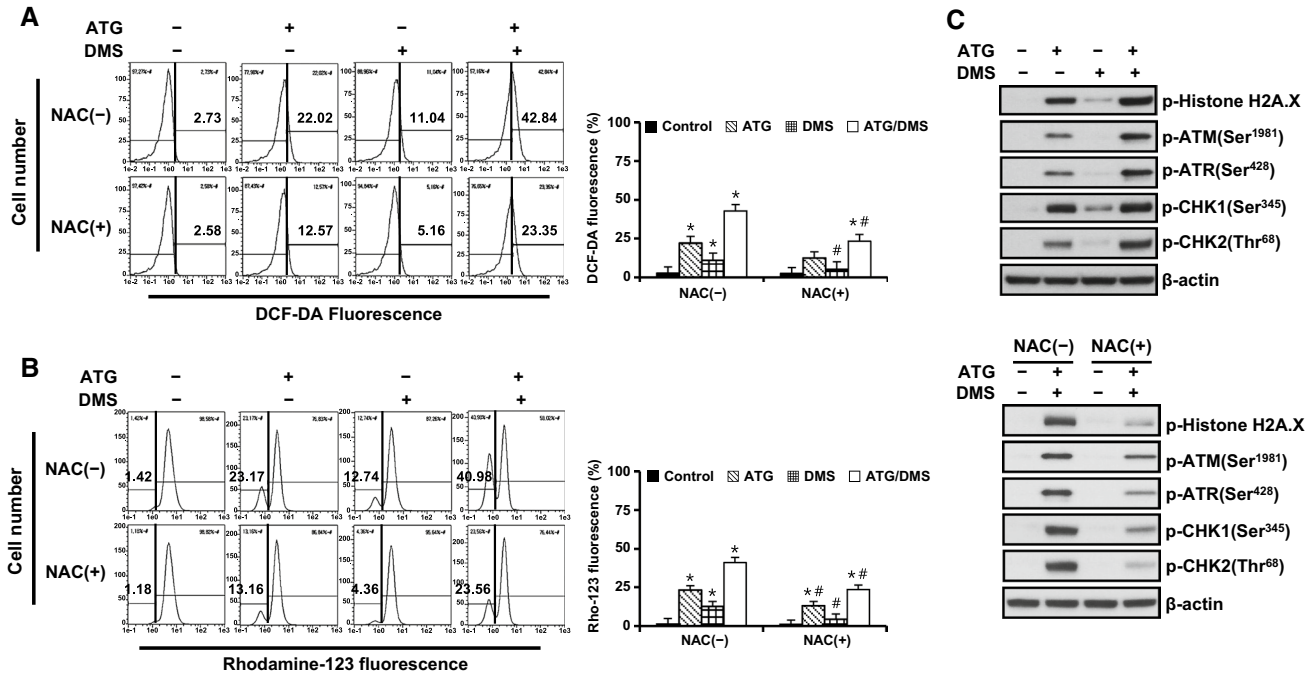

Fig. 5 Effects of pretreatment with *N*-acetylcysteine following combination treatment of arctigenin and dexamethasone on ROS, mitochondrial function, and DNA damage in RPMI-2650 cells. Cells were pretreated with *N*-acetylcysteine (5 mM) prior to treatment with ATG (5 μM) and DMS (12.5 μM) alone or in combination for 48 h. **a** Cellular ROS levels were measured after staining cells with DCF-DA (10 μM). **b** ΔΨm was measured after staining the cells with 30 nM of Rhodamine123. **c** Levels of apoptosis- and necroptosis-related proteins were measured by Western blotting. *ATG* arctigenin, *DMS* dexamethasone, *ATG/DMS* combination treatment of arctigenin and dexamethasone, *NAC* *N*-acetylcysteine. $^{*}P<0.05$ compared with respective controls. $^{\#}P<0.05$ compared with respective controls without NAC pretreatment

by significant decreases of cell viability, intracellular ATP levels and mitochondrial function. Mitochondrial apoptosis was evidenced by increased Bax/Bcl-2 ratio, the occurrence of sub-G_0/G_1 peak in flow cytometry, and increased cleaved form of caspase-3. The involvement of necroptosis was observed by increasing levels of p-RIP3 and p-MLKL. Concurrent induction of necroptosis and apoptosis was further confirmed by increases of annexin V-PE-positive/7-AAD-positive cells and annexin V-PE-positive/7-AAD-negative cells, respectively, in annexin V-PE binding assay. In addition, pharmacological inhibition of RIP1 and pan-caspases caused by necrostatin-1 and Q-VD-Oph-1, respectively, could reverse ATG/DMS-induced cytotoxicity. Drugs or natural compounds that can induce apoptosis or necroptosis in cancer cells have been well studied in various types of cancer cells. However, studies on the naturally occurring compounds showing simultaneous induction of apoptosis and necroptosis have only been reported in some substances including shikonin (Chen et al. 2017). Necroptosis, a subset of programmed necrosis, can be exploited to control against cancerous cells that are defective in apoptotic machinery (He et al. 2017a). Considering that resistance to apoptosis is a major cause of resistance to anticancer drugs, the development of agents targeting necroptosis pathways may provide novel opportunities to induce cancer cell death, especially for apoptosis-resistant forms of cancer.

Since spheroids mimic solid tumors rather than 2D monolayer cell cultures, they can be a very useful model for studying the mechanism of action of anticancer drugs in solid tumors. In 3D cultures treated with ATG/DMS, increased PI(+) areas showing necrotic cell death with decreased cell viability in spheroids were restored by pretreatment with antioxidant NAC. This is consistent with the results in 2D cultures. In particular, upregulation of mediators for apoptosis and necroptosis in spheroids confirms the results of 2D cell cultures in which ATG/DMS induced RPMI-2650 cell death through concurrent induction of apoptosis and necroptosis.

Oxidative stress is considered an imbalance in ROS production and their removal by antioxidants. It is a primary cause of damage to cellular components such as DNA, proteins, lipids, and membranes. Mitochondria are major intracellular source and target of ROS in most tissues (Chernyak et al. 2006). In our study, ATG/DMS increased the production of ROS with a significant loss in ΔΨm indicative of mitochondrial dysfunction. Pretreatment with antioxidant NAC can prevent them. It has been reported that the loss of ΔΨm can decrease the coupling efficiency of the electron

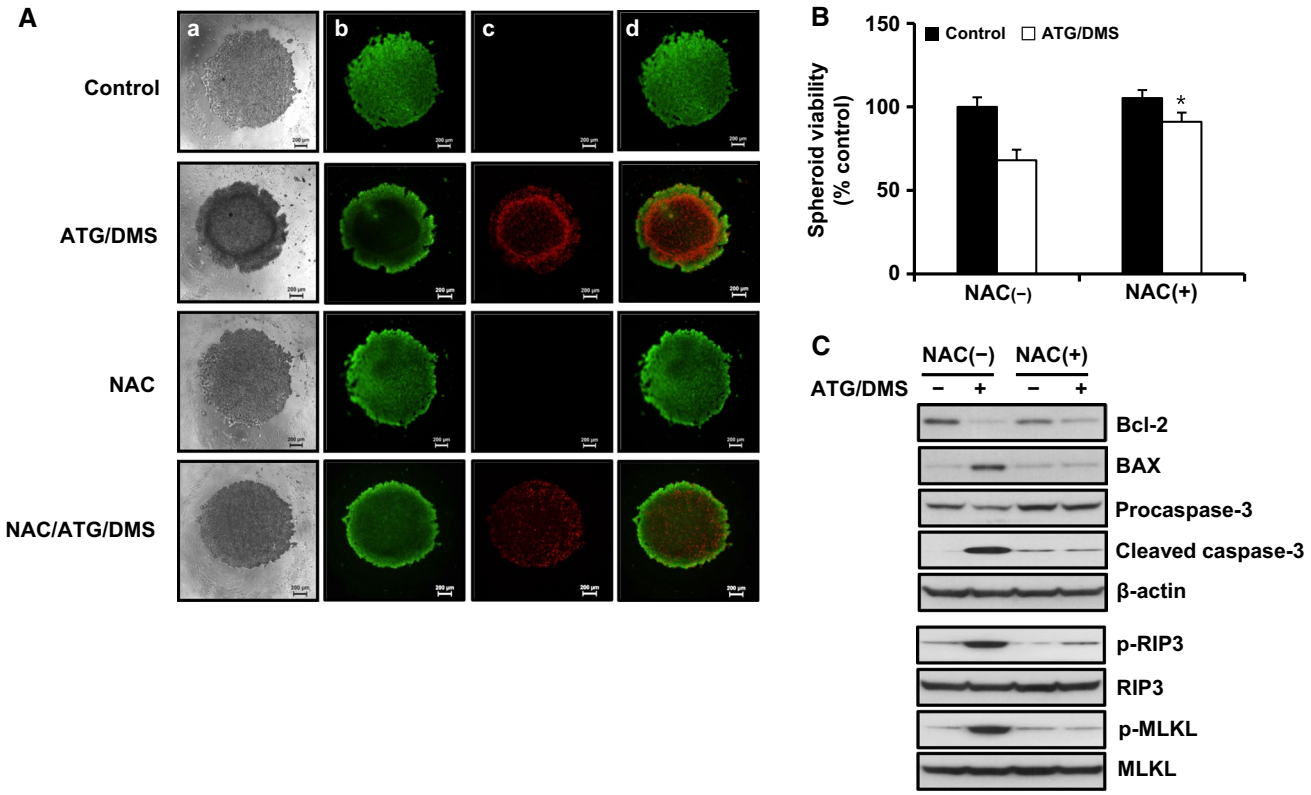

Fig. 6 Effects of pretreatment with *N*-acetylcysteine on arctigenin-promoted cytotoxicity in 3D culture of RPMI-2650 cells. Spheroids were cultured in Ultra Low cluster 96-well plate and pretreated with or without *N*-acetylcysteine (NAC, 5 mM) 2 h prior to treatment with ATG (5 μM) and DMS (12.5 μM) for another 48 h. **a** Vitality staining of RPMI-2650 spheroids [from left to right: phase-contrast image (a), fluorescent images of FDA(+) living cells in green (b), PI(+) dead cells in red (c), and merged (d)]. **b** Percentage of spheroid viability was determined using the Enhanced Cell Viability Assay kit. **c** The protein levels were assessed by Western blotting. *ATG* arctigenin, *DMS* dexamethasone, *ATG/DMS* combination treatment of arctigenin and dexamethasone. $*P < 0.05$ compared with respective controls without NAC pretreatment

transport chain, subsequently reducing the cellular ATP levels and contributing to cell death (Ricci et al. 2004). The reduction in cellular ATP levels found in this study supports an earlier report of ATP depletion due to inhibition of mitochondrial respiration by ATG (Gu et al. 2012). Furthermore, concurrent apoptosis and necroptosis following ATG/DMS suggest that a series of the cellular responses induced by the two compounds are associated with mitochondrial dysfunction. Mitochondria are essential for cellular energy balance which controls the progression of cell death. Mitochondrial dysfunction is involved in the progression of apoptosis or necroptosis through common signals such as ROS (Zou et al. 2015). Such signals are detectably associated with cellular ATP levels. In the current study, ATG/DMS clearly reduced cellular ATP levels, while ATP supplement restored cell viability as well as levels of apoptosis and necroptosis markers. These findings support previous evidence that cellular ATP levels can determine the fate of apoptosis or necrosis (Eguchi et al. 1997; Leist et al. 1997). In this regard, ATP plays an important role in protecting cells from programmed cell death.

Oxidative DNA damage and subsequent induction of apoptosis by ATG/DMS found in the present study have been observed in the anticancer effects of several chemotherapeutic drugs including cisplatin (Mizutani 2007). ROS is known to induce DNA damage and cause single or double strands breaks that can activate DNA damage responses to repair damaged DNA (Levine et al. 2017). Thus, the presence of DNA damage responses with cell cycle transition delay at G_2/M phase and apoptosis suggests that excessive DNA damage exceeding DNA repair ability might have occurred in RPMI-2650 cells treated with ATG/DMS.

Cancer cells are under oxidative stress, reflecting the altered redox balance. Thus, cancer cells are more susceptible to agents that can induce redox imbalance and increase oxidative stress, while normal cells are less sensitive to oxidative stress inducers due to low level of basal ROS and

high antioxidant capacity (He et al. 2017b). Due to biochemical differences between cancer cells and normal cells, pro-oxidant-based therapeutic strategies that can increase the level of ROS or inhibit antioxidant have been widely applied as a major or adjuvant method of cancer treatment. In this regard, since ATG/DMS increased ROS levels and caused marked cytotoxicity by simultaneously inducing apoptosis and necroptosis, making it a potential candidate in cancer treatment. The potential of ATG to sensitize cells to the cytotoxic effects of conventional chemotherapeutic drugs has been reported in several in vivo and in vitro studies (Lee et al. 2018; Wang et al. 2014; Yao et al. 2011). We have previously shown that combination treatment with ATG and docetaxel can cause preferential cytotoxicity to acidity-tolerant prostate carcinoma PC-3 cells and such effect is associated with ROS-mediated mitochondrial damage and inhibition of PI3 K/Akt/mTOR pathway (Lee et al. 2018). In addition, ATG has the potential to enhance chemosensitivity of cancer cells to cisplatin by reducing the amount of surviving (Wang et al. 2014) or inhibiting STAT3 signaling pathway (Yao et al. 2011). Gu et al. have reported that the combination treatment of ATG and 2-deoxyglucose can be a therapeutic strategy for cancer treatment by targeting cellular energy metabolism with minimum adverse effects on normal tissues (Gu et al. 2012).

Conclusion

Our results have demonstrated the efficacy of ATG as a therapeutic candidate in nasal septum carcinoma. To achieve better results, it can be combined with DMS. The role of necroptosis in the treatment of nasal septum carcinoma needs to be further investigated using animal models. Nevertheless, simultaneously targeting apoptosis and necroptosis in cancer might provide very promising opportunities for new drug development.

Acknowledgements The present study was supported by the Basic Science Research Program through the National Research Foundation (NRF) of Korea, funded by the Ministry of Education (No. NRF-2018R1D1A1B07046129).

Compliance with ethical standards

Conflict of interest Yoon-Jin Lee, Kwan-Sik Park, Byoung Joon Baek, Kyong-Ae Lee, and Sang-Han Lee declare that they have no conflict of interest.

Human and animal rights The article does not contain any studies with human and animal and this study was performed following institutional and national guidelines.

References

Allen MW et al (2008) Long-term radiotherapy outcomes for nasal cavity and septal cancers. Int J Radiat Oncol Biol Phys 71:401–406

Chambers KF, Mosaad EM, Russell PJ, Clements JA, Doran MR (2014) 3D Cultures of prostate cancer cells cultured in a novel high-throughput culture platform are more resistant to chemotherapeutics compared to cells cultured in monolayer. PLoS ONE 9:e111029

Chen C et al (2017) Shikonin induces apoptosis and necroptosis in pancreatic cancer via regulating the expression of RIP1/RIP3 and synergizes the activity of gemcitabine. Am J Transl Res 9:5507–5517

Chernyak BV et al (2006) Production of reactive oxygen species in mitochondria of HeLa cells under oxidative stress. Biochim Biophys Acta 1757:525–534

Davatgaran-Taghipour Y et al (2017) Polyphenol nanoformulations for cancer therapy: experimental evidence and clinical perspective. Int J Nanomed 12:2689–2702

Dorscheid DR et al (2001) Apoptosis of airway epithelial cells induced by corticosteroids. Am J Respir Crit Care Med 164:1939–1947

Eguchi Y, Shimizu S, Tsujimoto Y (1997) Intracellular ATP levels determine cell death fate by apoptosis or necrosis. Cancer Res 57:1835–1840

Feng T et al (2017) Arctigenin inhibits STAT3 and exhibits anticancer potential in human triple-negative breast cancer therapy. Oncotarget 8:329–344

Fradis M, Podoshin L, Gertner R, Sabo E (1993) Squamous cell carcinoma of the nasal septum mucosa. Ear Nose Throat J 72:217–221

Fujioka R et al (2018) Change in plasma lactate concentration during arctigenin administration in a phase I clinical trial in patients with gemcitabine-refractory pancreatic cancer. PLoS ONE 13:e0198219

Greenberg AK et al (2002) Glucocorticoids inhibit lung cancer cell growth through both the extracellular signal-related kinase pathway and cell cycle regulators. Am J Respir Cell Mol Biol 27:320–328

Gu Y et al (2012) Arctigenin preferentially induces tumor cell death under glucose deprivation by inhibiting cellular energy metabolism. Biochem Pharmacol 84:468–476

He GW et al (2017a) Regression of apoptosis-resistant colorectal tumors by induction of necroptosis in mice. J Exp Med 214:1655–1662

He L et al (2017b) Antioxidants maintain cellular redox homeostasis by elimination of reactive oxygen species. Cell Physiol Biochem 44:532–553

Ikeda M et al (2016) Phase I trial of GBS-01 for advanced pancreatic cancer refractory to gemcitabine. Cancer Sci 107:1818–1824

Ioannidis JP, Hesketh PJ, Lau J (2000) Contribution of dexamethasone to control of chemotherapy-induced nausea and vomiting: a meta-analysis of randomized evidence. J Clin Oncol 18:3409–3422

Lee YJ, Oh JE, Lee SH (2018) Arctigenin shows preferential cytotoxicity to acidity-tolerant prostate carcinoma PC-3 cells through ROS-mediated mitochondrial damage and the inhibition of PI3 K/Akt/mTOR pathway. Biochem Biophys Res Commun 505:1244–1250

Leist M et al (1997) Intracellular adenosine triphosphate (ATP) concentration: a switch in the decision between apoptosis and necrosis. J Exp Med 185:1481–1486

Levine AS et al (2017) The oxidative DNA damage response: a review of research undertaken with Tsinghua and Xiangya students at the University of Pittsburgh. Sci China Life Sci 60:1077–1080

Li M et al (2010) Dexamethasone enhances trichosanthin-induced apoptosis in the HepG2 hepatoma cell line. Life Sci 86:10–16

Li QC, Liang Y, Tian Y, Hu GR (2016) Arctigenin induces apoptosis in colon cancer cells through ROS/p38MAPK pathway. J BUON 21:87–94

McGuirt WF, Thompson JN (1984) Surgical approaches to malignant tumors of the nasal septum. Laryngoscope 94:1045–1049

Mizutani H (2007) Mechanism of DNA damage and apoptosis induced by anticancer drugs through generation of reactive oxygen species. Yakugaku Zasshi 127:1837–1842

Qin X et al (2019) The role of necroptosis in cancer: a double-edged sword? Biochim Biophys Acta Rev Cancer 1871:259–266

Ricci JE et al (2004) Disruption of mitochondrial function during apoptosis is mediated by caspase cleavage of the p75 subunit of complex I of the electron transport chain. Cell 117:773–786

Wang H et al (2007) Dexamethasone as a chemosensitizer for breast cancer chemotherapy: potentiation of the antitumor activity of adriamycin, modulation of cytokine expression, and pharmacokinetics. Int J Oncol 30:947–953

Wang HQ, Jin JJ, Wang J (2014) Arctigenin enhances chemosensitivity to cisplatin in human nonsmall lung cancer H460 cells through downregulation of survivin expression. J Biochem Mol Toxicol 28:39–45

Xu Y, Lou Z, Lee SH (2017) Arctigenin represses TGF-β-induced epithelial mesenchymal transition in human lung cancer cells. Biochem Biophys Res Commun 493:934–939

Yamamoto T et al (2002) Inhibition of murine osteosarcoma cell proliferation by gluocorticoid. Anticancer Res 22:4151–4156

Yao X et al (2011) Arctigenin enhances chemosensitivity of cancer cells to cisplatin through inhibition of the STAT3 signaling pathway. J Cell Biochem 112:2837–2849

Zhu P et al (2018) Ripk3 promotes ER stress-induced necroptosis in cardiac IR injury: a mechanism involving calcium overload/XO/ROS/mPTP pathway. Redox Biol 16:157–168

Zou X et al (2015) Inhibitory effects of 3-bromopyruvate in human nasopharyngeal carcinoma cells. Oncol Rep 34:1895–1904